Observation of chorus waves by the Van Allen Probes: dependence on solar wind parameters and scale size: Chorus wave distribution and scale size

Article *in* Journal of Geophysical Research: Space Physics · July 2016

DOI: 10.1002/2016JA022775

CITATIONS
27

READS
238

5 authors, including:

Homayon Aryan
University of California, Los Angeles
28 PUBLICATIONS **210** CITATIONS

SEE PROFILE

Oleksiy Agapitov
University of California, Berkeley
160 PUBLICATIONS **3,345** CITATIONS

SEE PROFILE

Craig A. Kletzing
University of Iowa
432 PUBLICATIONS **15,992** CITATIONS

SEE PROFILE

AGU PUBLICATIONS

JGR

Journal of Geophysical Research: Space Physics

RESEARCH ARTICLE

10.1002/2016JA022775

Key Points:
- Distribution of chorus wave intensities in the inner magnetosphere observed by the Van Allen Probes
- Scale size of chorus wave packets as a function of radial distance, magnetic latitude, and geomagnetic activity
- Distribution of chorus wave intensities as a function of combined geomagnetic and solar wind parameters

Correspondence to:
H. Aryan,
aryan.homayon@gmail.com

Citation:
Aryan, H., D. Sibeck, M. Balikhin, O. Agapitov, and C. Kletzing (2016), Observation of chorus waves by the Van Allen Probes: Dependence on solar wind parameters and scale size, *J. Geophys. Res. Space Physics*, *121*, 7608–7621, doi:10.1002/2016JA022775.

Received 1 APR 2016
Accepted 24 JUL 2016
Accepted article online 28 JUL 2016
Published online 13 AUG 2016

Observation of chorus waves by the Van Allen Probes: Dependence on solar wind parameters and scale size

Homayon Aryan[1], David Sibeck[1], Michael Balikhin[2], Oleksiy Agapitov[3,4], and Craig Kletzing[5]

[1]NASA Goddard Space Flight Center, Greenbelt, Maryland, USA, [2]Department of Automatic Control and Systems Engineering, University of Sheffield, Sheffield, UK, [3]Space Sciences Laboratory, University of California, Berkeley, California, USA, [4]Astronomy and Space Physics Department, Taras Shevchenko National, University of Kiev, Kiev, Ukraine, [5]Department of Physics and Astronomy, University of Iowa, Iowa City, Iowa, USA

Abstract Highly energetic electrons in the Earth's Van Allen radiation belts can cause serious damage to spacecraft electronic systems and affect the atmospheric composition if they precipitate into the upper atmosphere. Whistler mode chorus waves have attracted significant attention in recent decades for their crucial role in the acceleration and loss of energetic electrons that ultimately change the dynamics of the radiation belts. The distribution of these waves in the inner magnetosphere is commonly presented as a function of geomagnetic activity. However, geomagnetic indices are nonspecific parameters that are compiled from imperfectly covered ground based measurements. The present study uses wave data from the two Van Allen Probes to present the distribution of lower band chorus waves not only as functions of single geomagnetic index and solar wind parameters but also as functions of combined parameters. Also the current study takes advantage of the unique equatorial orbit of the Van Allen Probes to estimate the average scale size of chorus wave packets, during close separations between the two spacecraft, as a function of radial distance, magnetic latitude, and geomagnetic activity, respectively. Results show that the average scale size of chorus wave packets is approximately 1300–2300 km. The results also show that the inclusion of combined parameters can provide better representation of the chorus wave distributions in the inner magnetosphere and therefore can further improve our knowledge of the acceleration and loss of radiation belt electrons.

1. Introduction

Plasma waves within the inner magnetosphere play an important role in the dynamics of the radiation belts [*Bortnik and Thorne*, 2007; *Thorne*, 2010; *Shprits et al.*, 2013]. They are observed in different regions with various frequency domains and are studied by various satellites such as the Van Allen Probes [*Santolík et al.*, 2014; *Li et al.*, 2014], THEMIS (Time History of Events and Macroscale Interactions during Substorms) [*Li et al.*, 2009; *Meredith et al.*, 2012], Cluster [*Santolík et al.*, 2004; *Yearby et al.*, 2011; *Agapitov et al.*, 2011; *Meredith et al.*, 2012; *Agapitov et al.*, 2013], CRRES (Combined Release and Radiation Effects Satellite) [*Meredith et al.*, 2003, 2012], Double Star [*Aryan et al.*, 2014], Polar [*LeDocq et al.*, 1998; *Santolík et al.*, 2010; *Tsurutani et al.*, 2012], and Geotail [*Yagitani et al.*, 2014]. One of the most conspicuous is the discrete chorus emission, which is a very intense right hand polarized electromagnetic whistler mode wave. Chorus waves are excited naturally in the low-density region within a few degrees of the geomagnetic equator outside the plasmapause [*Burtis and Helliwell*, 1969; *LeDocq et al.*, 1998; *Santolík et al.*, 2005; *Agapitov et al.*, 2010]. They are observed as short coherent bursts in two separate frequency bands: the lower band ($0.1f_{ce} < f < 0.5f_{ce}$) and the upper band ($0.5f_{ce} < f < f_{ce}$) with a gap in wave power at 0.5 f_{ce} [*Burtis and Helliwell*, 1969; *Helliwell*, 1967; *Tsurutani and Smith*, 1974], where f_{ce} is the electron gyrofrequency ($f_{ce} = eB/m_e$). Cyclotron resonance with anisotropic energetic electrons injected from the plasma sheet is thought to be responsible for the excitation of chorus waves [*Kennel and Petschek*, 1966; *Meredith et al.*, 2000; *Omura et al.*, 2009] that will subsequently propagate from equatorial regions to higher latitudes in both the Southern and the Northern hemispheres [*LeDocq et al.*, 1998; *Santolík and Gurnett*, 2003; *Bortnik and Thorne*, 2007; *Santolík et al.*, 2014].

Substorms and enhanced convection events transport energetic electrons into geosynchronous orbit [*Li and Cho*, 1997]. This process creates seed (tens to hundreds of keV) electrons, which form an important

source of energetic electrons in the radiation belts. Local acceleration by wave particle interactions [*Summers et al.*, 2002; *Thorne et al.*, 2005; *Horne et al.*, 2005] through efficient energy diffusion [*Horne and Thorne*, 1998; *Summers et al.*, 2002] can further energize the seed electrons to highly relativistic energies [*Horne and Thorne*, 2003; *Baker and Kanekal*, 2008; *Thorne*, 2010]. In fact, during storm recovery phase, electron acceleration by chorus waves can increase the energetic electron flux in the radiation belts by 3 orders of magnitude over prestorm values [*Summers et al.*, 1998; *Meredith et al.*, 2003; *Horne et al.*, 2005; *Thorne et al.*, 2013; *Reeves et al.*, 2013]. In addition, combined acceleration by chorus and magnetosonic waves can yield an unusual butterfly distribution of relativistic electrons well inside of geostationary orbit [*Xiao et al.*, 2015].

Chorus is also the dominant scattering process leading to diffuse auroral precipitation [*Ni et al.*, 2008; *Thorne*, 2010] and it has been shown that lower band chorus is the driver of the pulsating aurora [*Nishimura et al.*, 2010, 2011]. Additionally, evidence points to whistler mode chorus as an important source of plasmaspheric hiss [*Bortnik et al.*, 2009; *Meredith et al.*, 2013; *Bortnik et al.*, 2016], which is responsible for both the formation of the slot region [*Lyons et al.*, 1972; *Lyons and Thorne*, 1973; *Abel and Thorne*, 1998], and also responsible for the decay of energetic electrons in the outer radiation belt during relatively quiet times [*Summers et al.*, 2007] due to resonant pitch angle scattering of energetic electrons [*Lyons et al.*, 1972]. According to a detailed ray tracing by *Bortnik et al.* [2008], a fraction of the chorus wave energy can propagate from an equatorial source region ($4 < L < 7$) outside the plasmasphere to high latitudes and subsequently refract into the plasmasphere, where it blends into the incoherent band of plasmaspheric hiss.

Rightfully, whistler mode chorus waves have attracted significant attention in recent decades for their crucial role in the acceleration and loss of energetic electrons [*Bortnik and Thorne*, 2007; *Shprits et al.*, 2009; *Baker et al.*, 2014] that ultimately change the dynamics of the radiation belts [*Meredith et al.*, 2002, 2003; *Li et al.*, 2009; *Xiao et al.*, 2009, 2010; *Thorne*, 2010; *Thorne et al.*, 2010; *Li et al.*, 2011; *Meredith et al.*, 2012; *Li et al.*, 2014]. The distribution of chorus waves in the inner magnetosphere is commonly presented as a function of geomagnetic activity [*Meredith et al.*, 2004; *Li et al.*, 2009, 2011; *Meredith et al.*, 2012; *Agapitov et al.*, 2015]. However, geomagnetic indices are compiled from imperfectly covered ground based measurements [*Weygand and Zesta*, 2008]. Although geomagnetic indices are principally continuous and homogeneous over long time periods, they are indirect and nonspecific parameters [*Baker et al.*, 1990; *Turner et al.*, 2000]. In general, geomagnetic indices indicate the solar wind changes that ultimately drive energetic electron enhancements [*Baker et al.*, 1990]. Recently, *Aryan et al.* [2014] used the Double Star wave data to show that chorus emissions depend on both geomagnetic activity and solar wind parameters.

The present study uses wave data from the two Van Allen Probes to present the distribution of lower band chorus waves not only as functions of single geomagnetic index and solar wind parameters but also as functions of combined geomagnetic index and solar wind parameters. Furthermore, chorus emissions contain many distinct nonlinear wave packets with changing frequency. Individual chorus elements, in terms of frequency change with time, can be classified into intense short duration (typically 10^{-1} s) rising tone, falling tone, hooks, flat types, and triggered emissions [*Burtis and Helliwell*, 1976; *Sazhin and Hayakawa*, 1992]. Groups of chorus elements within an individual wave packet pulsate with a periodicity of approximately 10 s and may be generated at random places over a broader source region [*Santolík et al.*, 2004; *Nishimura et al.*, 2011] close to the magnetic equatorial plane [*Helliwell*, 1967; *LeDocq et al.*, 1998; *Santolík*, 2008], where the central position of the chorus source fluctuates at time scale of minutes within 1000–2000 km of the geomagnetic equator [*Santolík et al.*, 2004]. While the location of chorus wave source region [*LeDocq et al.*, 1998; *Inan et al.*, 2004; *Santolík*, 2008; *Santolík et al.*, 2010] has been explored thoroughly, there are some uncertainty in the scale size of chorus wave packets. According to *Santolík and Gurnett* [2003], the dimension of the chorus source regions measured along the magnetic field lines is 3000–5000 km based on Poynting flux and polarization measurements by the STAFF-SA instruments [*Cornilleau-Wehrlin et al.*, 2005] on board the Cluster spacecraft. More recently, *Agapitov et al.* [2010] evaluated the Poynting flux and wave vector distributions by the search coil magnetometer observations [*Le Contel et al.*, 2008] on board THEMIS to show that the dimension of the chorus source scale transverse to the local magnetic field to be in the 2800–3200 km range. In addition, *Nishimura et al.* [2011] estimated the transverse scale size of coherently pulsating chorus patches to be in the range of several thousands of kilometers, with the aid of all sky imagers.

The current study estimates the scale sizes of chorus wave packets using the two Van Allen Probes during close separations between the two spacecraft as a function of radial distance (L), magnetic latitude (λ), and geomagnetic activity (AE), respectively. The orbit of the two Van Allen Probes is designed such that roughly

every 69 days, the separation distances between the two spacecraft vary between approximately 55 km and 4.4×10^4 km. This unique equatorial orbit of the Van Allen Probes provides the platform to study scale sizes of chorus wave packets in more detail in order to understand the interaction region better and allow us to compare theoretical predictions with the observations.

2. Data

The two identical Van Allen Probes, launched on 30 August 2012, operate in almost identical orbits with a perigee of approximately 1.1 R_E, an apogee of 5.8 R_E geocentric, and an inclination of 10° [*Mauk et al.*, 2013] allowing the Van Allen Probes to access all of the most critical regions of the radiation belts. Aboard each Van Allen Probe, the Waveform Receiver (WFR) on the EMFISIS (Electric and Magnetic Field Instrument Suite and Integrated Science) waves instrument measures wave power spectral density between 10 Hz and 12 kHz [*Kletzing et al.*, 2013; *Wygant et al.*, 2013]. The EMFISIS instrument suite measures the background magnetic fields by a triaxial fluxgate magnetometer and wave magnetic field fluctuations by a triaxial search coil magnetometer [*Kletzing et al.*, 2013]. A comprehensive set of wave electric and magnetic field measurements is processed by the EMFISIS waves instrument, thus enabling comprehensive measurements of chorus waves. This study uses almost 3 years (from September 2012 to end of May 2015) of EMFISIS waves data on board the two Van Allen Probes.

Relativistic electrons interact more readily with lower band chorus in the frequency range of $0.1f_{ce} \leq f \leq 0.5f_{ce}$ [*Horne and Thorne*, 1998]. Therefore, for the study of chorus wave distributions the wave spectral intensity ($pT^2\ Hz^{-1}$) is integrated over the lower band chorus frequency range ($0.1f_{ce} \leq f \leq 0.5f_{ce}$) to obtain the lower band chorus magnetic field intensities, ${B_w}^2$, where B_w is the magnetic field amplitude. The data are selected only in the cases where the wave frequencies are within the range $0.1f_{ce} \leq f \leq 0.5f_{ce}$ [*Meredith et al.*, 2001, 2012] and in the low-density region outside the plasmapause [*Sheeley et al.*, 2001].

The second part of this study uses the 3-D magnetic field waveforms from search coil magnetometers which have been captured in a continuous waveform burst mode with selected 6 s snapshots from search coil magnetometers. We select chorus elements with frequencies in the range of $0.1f_{ce} \leq f \leq 0.5f_{ce}$ and in the low-density region outside the plasmapause [*Sheeley et al.*, 2001]. We then perform Hilbert transform on the waveform data to obtain wave amplitudes (B) for all identified chorus elements. The difference in wave amplitude (ΔB) observed by each of the two spacecraft for the selected events is then grouped in 10 km S_d bins (where S_d is the separation distance between the two spacecraft). We then plot ΔB versus S_d and use these plots to estimate the chorus scale size as a function of radial distance, magnetic latitude, and geomagnetic activity, respectively.

The geomagnetic index (AE) and the solar wind parameters (southward interplanetary magnetic field (B_s), where B_s is the negative component of B_z (i.e., $B_s = -B_z$ for $B_z < 0$), and velocity (V) used in this study was obtained by NASA's Goddard Space Flight Center (GSFC) SPDF OMNIWEB [*King and Papitashvili*, 2005] using data from Wind and ACE spacecraft and is available online with relatively high resolution (1 min). The data are binned in linear steps of 0.1 L and 1 h MLT (magnetic local time). The geomagnetic activity is split into three intervals which are defined as quiet when $AE < 100$ nT, moderate when $100 \leq AE \leq 500$ nT, and active when $AE > 500$ nT. The solar wind velocity is also split into three intervals which are defined as slow when $V < 400$ km/s, moderate when $400 \leq V \leq 600$ km/s, and fast when $V > 600$ km/s. Similarly, the B_s is split into three intervals which are defined as low when $B_s < 4$ nT, moderate when $4 \leq B_s \leq 8$ nT, and high when $B_s > 8$ nT.

3. Results and Discussions

3.1. Distribution of Chorus Waves in the Inner Magnetosphere

Many studies have shown that the intensities of lower band chorus emissions depend on geomagnetic activity, where the largest peak chorus intensities are observed during active conditions, primarily, in the region of $4 \leq L \leq 9$ from 2300 MLT to 1300 MLT [*Meredith et al.*, 2004; *Li et al.*, 2009, 2011; *Meredith et al.*, 2012; *Agapitov et al.*, 2013; *Aryan et al.*, 2014]. However, geomagnetic indices are indirect parameters that are compiled from imperfectly covered ground based measurements. For example, the AE index is compiled from the magnetograms of several auroral zone observatories to represent auroral electrojet properties [*Davis and Sugiura*, 1966]. Despite its universal use in wave models, the AE index may not always be able to monitor the electrojet activity precisely [*Akasofu et al.*, 1973; *Lui et al.*, 1976] due to the highly variable auroral ovals

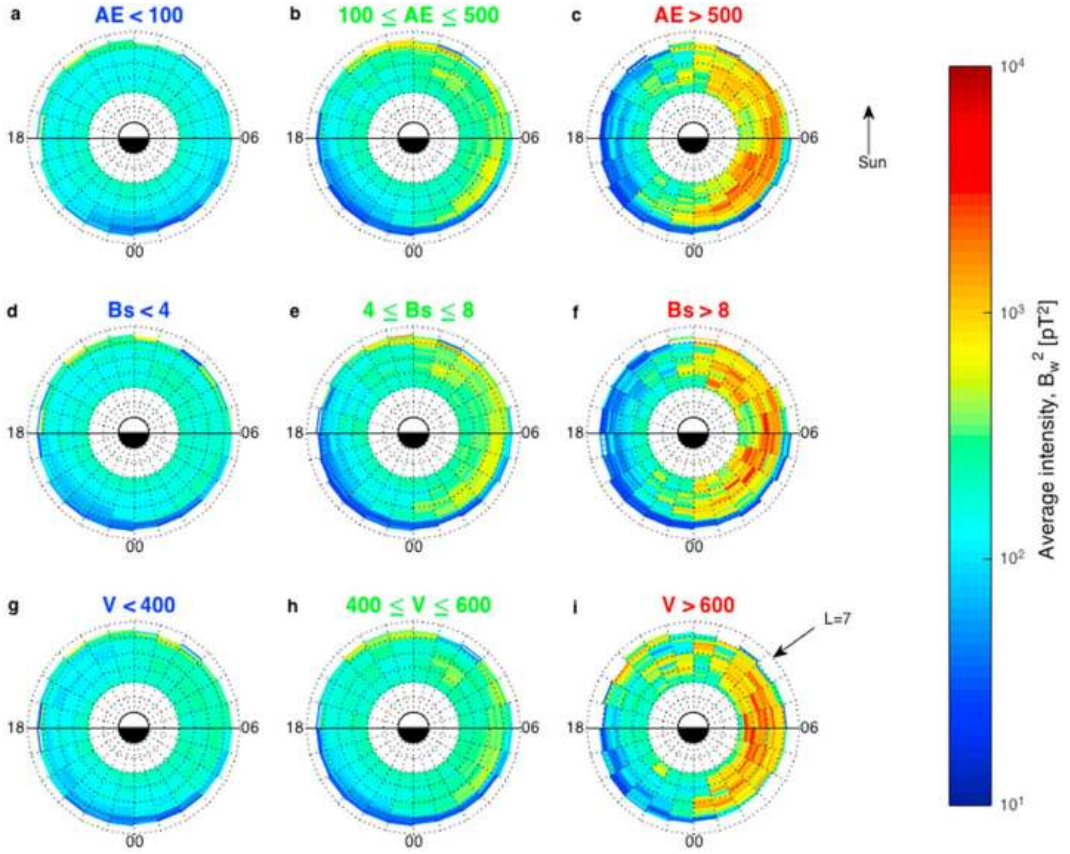

Figure 1. The (a–c) average lower band chorus intensities observed by Van Allen Probes as a function of *L*, MLT, and geomagnetic activity during quiet (a), moderate (b), and active (c) conditions. The (d–f) average lower band chorus intensities as a function of *L*, MLT, and southward interplanetary magnetic field for low (d), moderate (e), and high (f) B_s. The (g–i) average lower band chorus intensities as a function of *L*, MLT, and solar wind velocity during slow (g), moderate (h), and fast (i) velocities.

[*Hoffman and Burch*, 1973; *Lui et al.*, 1975; *Kamide and Winningham*, 1977]. Meanwhile, the planetary *Kp* index is derived from the subauroral *K* index measurements obtained from various midlatitude ground based magnetometer stations [*Menvielle and Berthelier*, 1991] to describe the geomagnetic disturbance. However, the subauroral stations are largely sensitive to convection due to the effects of the inner edge of the plasma sheet [*Thomsen*, 2004], which may introduce ambiguities in its interpretations [*Wing et al.*, 2005]. Similarly, the *Dst* index is developed from low-latitude horizontal component magnetograms in an effort to determine the ring current strengths [*Sugiura*, 1963; *Turner et al.*, 2000]. Although the ring current is the most significant contributing current system in *Dst* index [*Roeder et al.*, 1996; *Hamilton et al.*, 1988; *Jordanova et al.*, 1998], it is possible that other low-latitude current systems, such as substorm induced currents, magnetotail currents, and induced currents in the solid Earth may also contribute to the *Dst* index [*Rostoker et al.*, 1997; *Turner et al.*, 2000]. In addition, not all geomagnetic storms necessarily change the flux of relativistic electrons in the outer radiation belt as it was shown by *Reeves et al.* [2003]. Therefore, it is important to use alternative parameters, such as the solar wind parameters and use multiple parameters in order to improve distribution models. Solar wind parameters are directly measured and more reliable. Solar wind velocity and southward interplanetary magnetic field are known to be effective in the control of electron fluxes. The flux enhancement in the outer belt is controlled by the interplanetary magnetic field sector polarity via the Russell-McPherron [*Russell and McPherron*, 1973] effect. Russell-McPherron effect strongly controls whether or not a given high speed stream is geoeffective. According to Russell-McPherron effect, the probability of southward interplanetary magnetic field increases when the angle θ (between the *z* axis in the GSM coordinate system and the *y* axis in the GSEQ coordinates system) decreases; thus, the southward interplanetary magnetic field is very important.

Figure 1 illustrates the average lower band chorus intensities observed by Van Allen Probes as functions of *L*, MLT, and geomagnetic activity during quiet (a), moderate (b), and active (c) conditions; southward

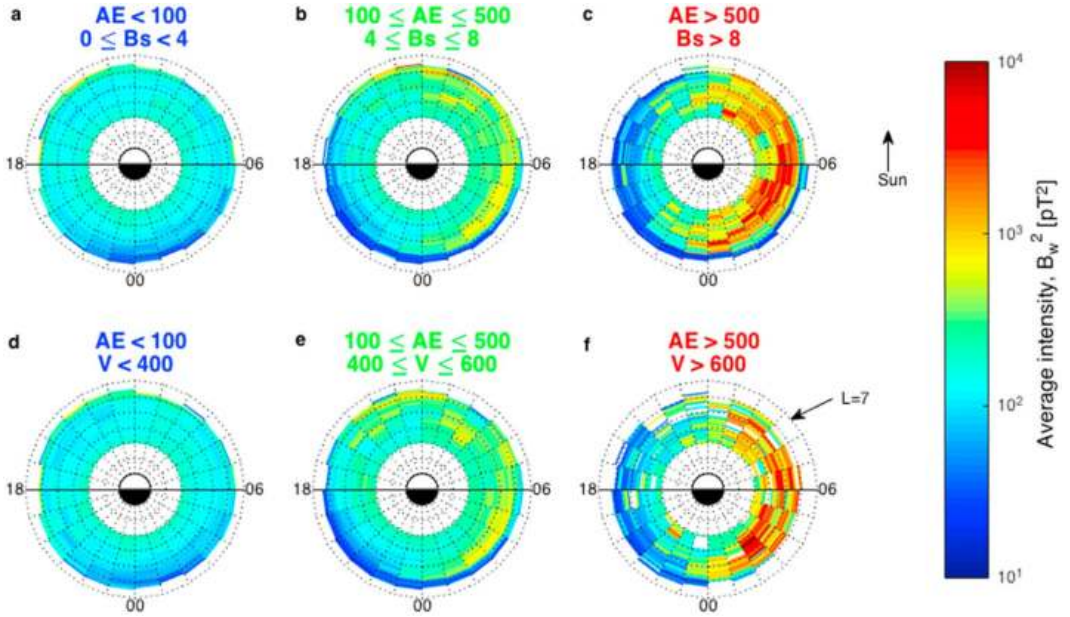

Figure 2. The average lower band chorus intensities observed by Van Allen Probes as functions of *L*, MLT for geomagnetic activity and (a–c) B_s, and (d–f) solar wind velocity (caption of Figure 1 applies).

interplanetary magnetic field (Bs) for low (d), moderate (e), and high (f) B_s; solar wind velocity during slow (g), moderate (h), and fast (i) velocities. It is commonly accepted that there is a time delay between changes in the solar wind parameters at L1 and the temporal changes observed in the inner magnetosphere [*Li et al.*, 2005; *Boynton et al.*, 2011; *Reeves et al.*, 2011; *Aryan et al.*, 2013]. Therefore, appropriate time delays were calculated using Kullback-Leibler theory [*Kullback and Leibler*, 1951; *Kullback*, 1959; *Aryan et al.*, 2014] for the solar wind parameters (B_s and *V*). The Kullback-Leibler theory calculates the difference between two probability distributions, which is known as the Kullback-Leibler distance, D_{KL} [*Aryan et al.*, 2014, equation (1)]. The distribution of chorus waves is divided under three different solar wind conditions (low, moderate, and high) for each solar wind parameter as shown in Figure 1. The Kullback-Leibler theory is applied by calculating D_{KL} between low and high (D_{KLlh}), low and moderate (D_{KLlm}), and moderate and high (D_{KLmh}) distributions. This is repeated for different time delays of up to 48 h at a 15 min time interval. The distribution for a particular time delay is deemed valid only if $D_{KLlh} > D_{KLlm}$ and $D_{KLlh} > D_{KLmh}$. Amongst the valid distributions, the largest D_{KLlh} represents the distribution with the best time delay.

Figure 1 illustrates that chorus emissions depend on geomagnetic activity and solar wind parameters. The largest peak chorus intensities in the order of 50 pT are observed during active conditions, high B_s, and fast solar wind velocities in the region of $3.5 < L < 6$ from 2300 MLT to 1300 MLT. These results are largely consistent with those from previous studies [e.g., *Li et al.*, 2009, 2011; *Meredith et al.*, 2012; *Aryan et al.*, 2014] that have presented the distribution of chorus waves in the inner magnetosphere as functions of geomagnetic activity or solar wind parameters. However, the models in Figure 1 are all based on a single geomagnetic index or solar wind parameter. As discussed above the geomagnetic indices are indirect and nonspecific, while the solar wind parameters observed at L1 may not impact the magnetosphere and vice versa. Therefore, a model based on a combination of geomagnetic index and solar wind parameter should mitigate possible errors and result in a better representation of chorus wave distributions in the inner magnetosphere. Figure 2 illustrates the average lower band chorus intensities observed by Van Allen Probes as functions of *L*, MLT for geomagnetic activity and B_s (Figures 2a–2c), and solar wind velocity (Figures 2d–2f). Results show that the largest peak chorus intensities are observed during active conditions and high B_s and active conditions and fast solar wind velocities in the region of $3.5 < L < 6$ from 2300 MLT to 1300 MLT. Results show that the peak chorus intensities of the combined parameter distributions model (Figure 2) are larger than those of the single parameter distributions model (Figure 1). In fact, the average peak intensities of the combined geomagnetic index and B_s model during active conditions and high B_s (Figure 2c) is 14% larger than the average peak intensities of the single parameter geomagnetic index during active conditions (Figure 1c). Similarly, the average peak intensities of the combined geomagnetic index and solar wind velocity model during active conditions and fast

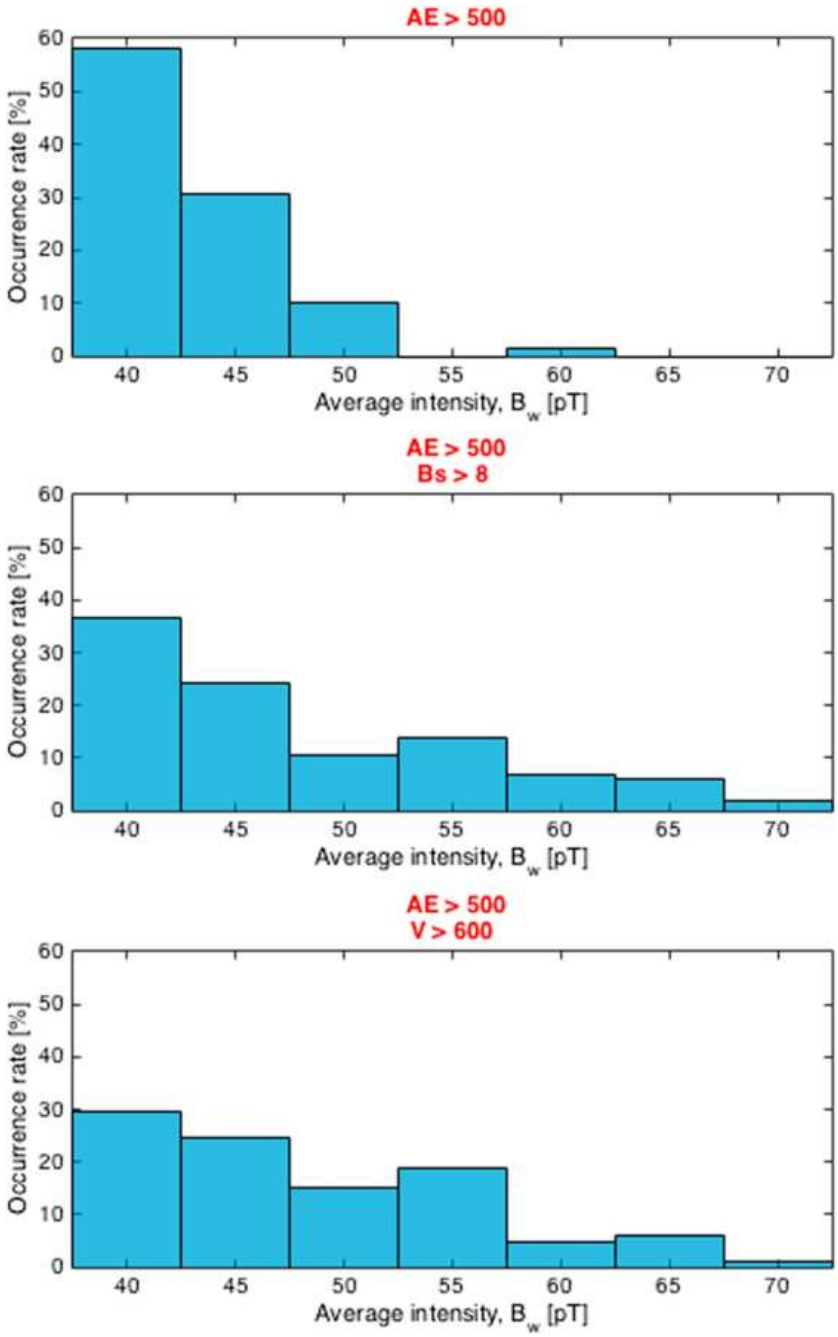

Figure 3. The peak average lower band chorus intensities for (top) $AE > 500$, (middle) $AE > 500$ and $B_s > 8$, and (bottom) $AE > 500$ and $V > 600$.

velocities (Figure 2f) are 17% larger than the average peak intensities of the single parameter geomagnetic index during active conditions (Figure 1c). Figure 3 shows a histogram of the peak average lower band chorus intensities for (top) $AE > 500$, (middle) $AE > 500$ and $B_s > 8$, and (bottom) $AE > 500$ and $V > 600$. It is clear that the peak average intensities for the *AE* parameter model are largely between 40 pT and 50 pT. In contrast, the peak average chorus intensities for the combined parameters extend from 40 pT to 70 pT. This shows that the single parameter *AE* model alone can underestimate the average chorus intensities. Therefore, it is important to take into account the effect of solar wind parameters not only because the combination of geomagnetic index and solar wind parameters provide better representation of chorus wave distributions but also because solar wind parameters are directly measured and more specific parameters. This can benefit studies of electron interaction with plasma waves, improve models that rely on the knowledge of chorus activity in the inner

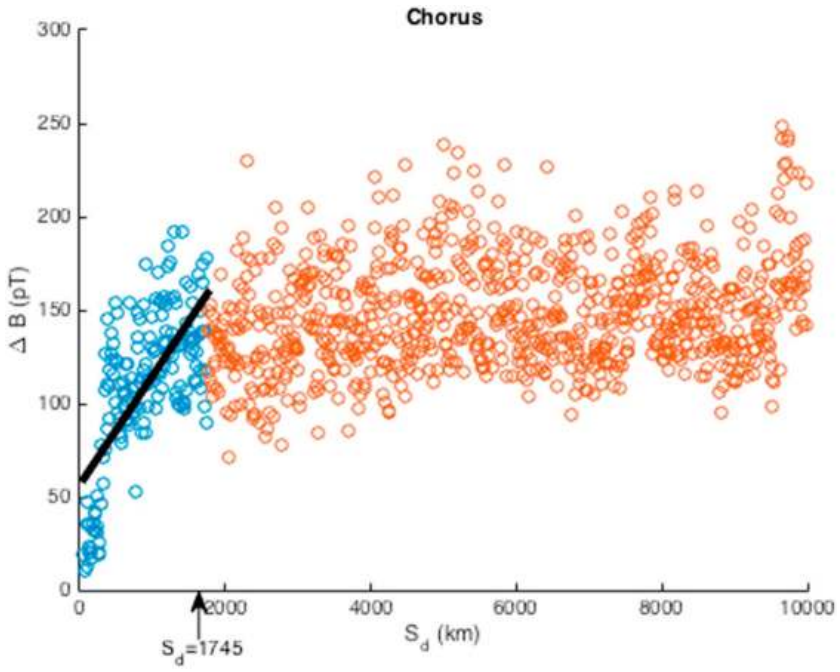

Figure 4. The difference between chorus wave amplitude (ΔB) observed by the two Van Allen Probes over different separation distances. Linear data are marked with blue circles, nonlinear data are marked with red circles, and the black line is the line of best fit.

magnetosphere (e.g., the Comprehensive Inner Magnetosphere-Ionosphere (CIMI) model) [*Fok et al.*, 2014], and therefore improve our knowledge of the acceleration and loss of radiation belt electrons.

3.2. Scale Size of Chorus Wave Packets

The separation distance between the two Van Allen Probes varies periodically between approximately 55 km and 4.4×10^4 km. When the two spacecraft are closely separated within the same chorus wave activity region, they may observe similar wave amplitudes and/or fluctuations that may be related to the same/similar chorus wave packets. This provides a unique opportunity to study chorus wave packets in more detail and try to estimate their scale sizes. The current study examines observations of chorus waves by the Van Allen Probes during close separations, up to 10,000 km. Figure 4 shows the difference between chorus wave amplitude (ΔB) observed by the two spacecraft over different separation distances (S_d). It is clear that ΔB is small when S_d is small, i.e., the two spacecraft are observing the same/similar chorus wave packets when they are close together. ΔB and S_d increase linearly (marked with blue circles) up to a saturation point (SP). Beyond the saturation point there is no relationship between ΔB and S_d (marked with red circles), i.e., the two spacecraft do not observe the same/similar chorus wave packets. Hence, the saturation point marks the transition point between the linear and nonlinear part of the plot, which is estimated to occur at around 1745 km using the reverse arrangement test [*Bendat and Piersol*, 2000; *Beck et al.*, 2006; *Aryan et al.*, 2013]. The separation distance where the saturation point occur is used as an estimate for the average scale size of chorus wave packets, which in this case it is approximately 1745 km. The black line with a correlation coefficient of 0.058 represents the line of best fit for the linear section of data.

The current study examines how the scale size of chorus wave packets may vary with radial distance, magnetic latitude, and geomagnetic activity (*AE*), respectively. Figure 5 shows the difference between chorus wave amplitude (ΔB) observed by the two spacecraft over different separation distances as a function of L in the region of (a) $3.0 \leq L < 4.0$, (b) $4.0 \leq L < 5.0$, and (c) $5.0 \leq L < 6.0$. Results show that at higher L the scale size of chorus wave packets is smaller than at lower L, as indicated by the saturation points (marked with arrows, from Figures 5a to 5c, 2265 km, 1745 km, and 1315 km), resulting in steeper line of best fit at higher L (the correlation coefficients, from Figures 5a to 5c, are 0.0593, 0.0868, and 0.0895). This means that at lower L the two spacecraft are more likely to observe the same/similar chorus wave packets over a larger S_d than at higher L. Beyond the saturation point ΔB is approximately 115 ± 10 pT in all four cases.

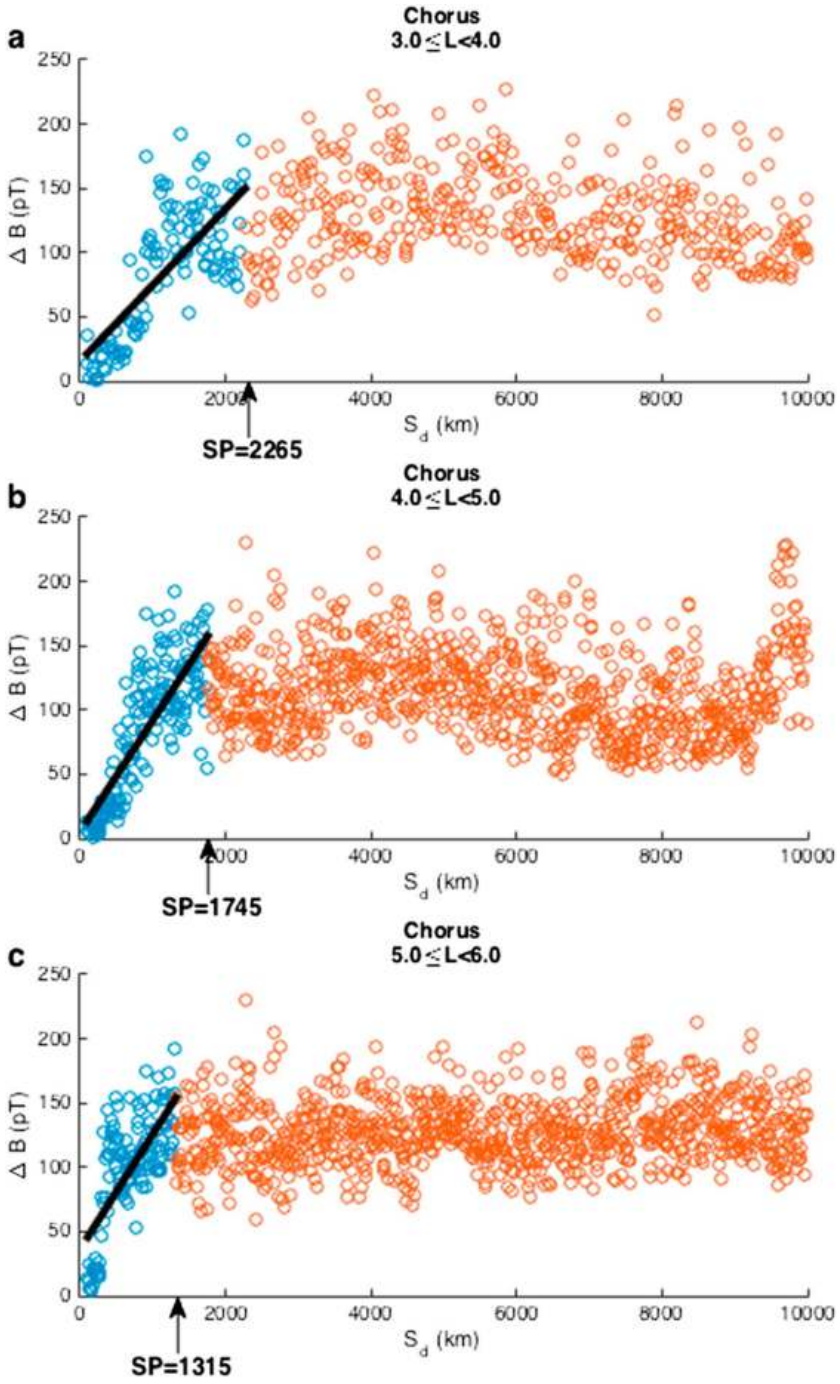

Figure 5. The difference between chorus wave amplitude (ΔB) observed by the two Van Allen Probes over different separation distances (S_d) as a function of L in the region of (a) $3.0 \leq L \leq 4.0$, (b) $4.0 \leq L \leq 5.0$, and (c) $5.0 \leq L \leq 6.0$ (caption of Figure 4 applies).

Chorus wave emissions also depend on magnetic latitude. They are excited naturally in the low-density region within a few degrees of the geomagnetic equator outside the plasmapause [*Burtis and Helliwell*, 1969; *LeDocq et al.*, 1998; *Santolík et al.*, 2005; *Agapitov et al.*, 2010] then they propagate to higher latitudes in both the Northern and Southern hemispheres. Figure 6 illustrates the difference between the wave amplitude observed by the two spacecraft over different separation distances as a function of magnetic latitude for (a) equatorial ($0° \leq \lambda < 5°$), (b) midlatitude ($5° \leq \lambda < 10°$), and (c) high latitude ($\lambda \geq 10°$). Results show that at high latitude the scale size of chorus wave packets is smaller than at the equator and midlatitude (marked with

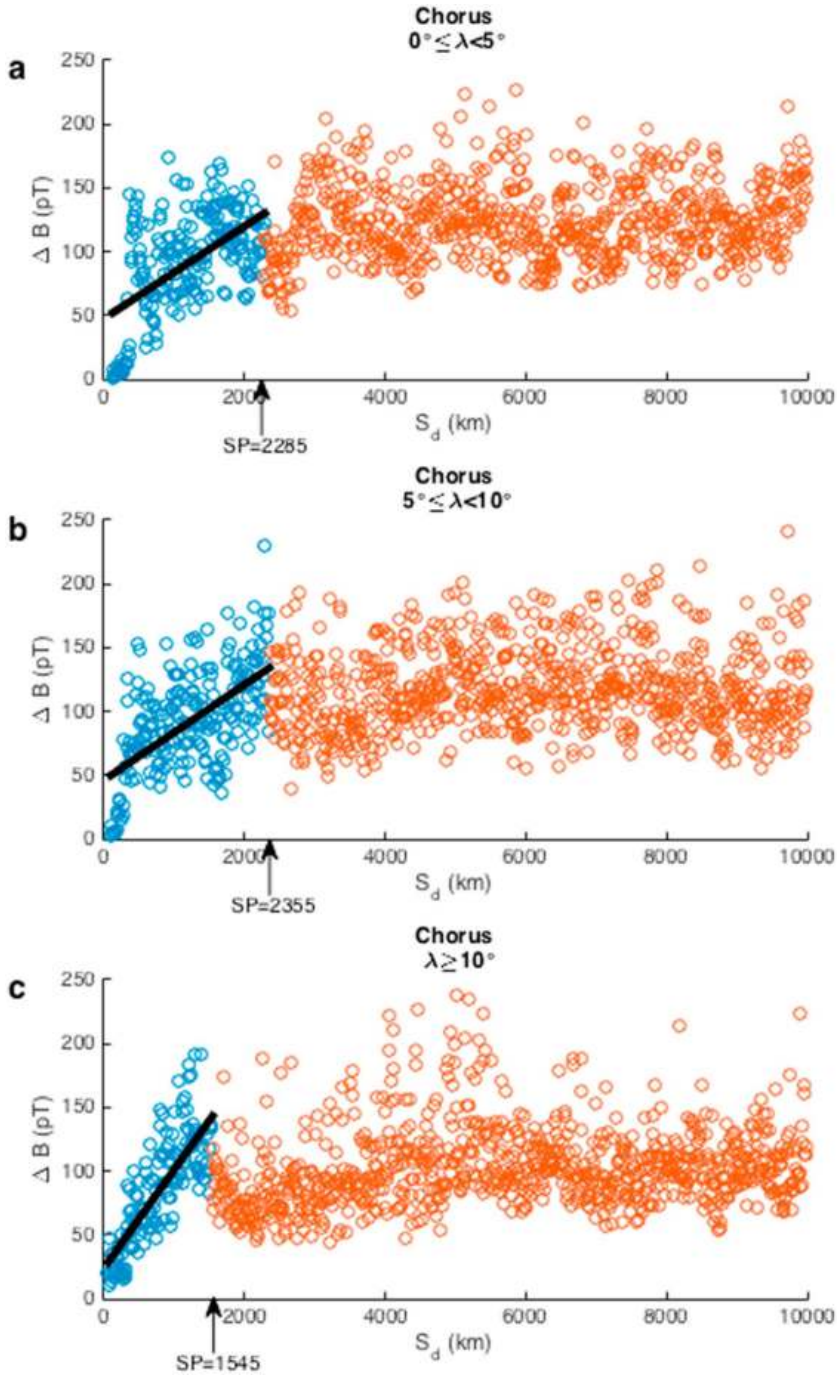

Figure 6. The difference between chorus wave amplitude (ΔB) observed by the two Van Allen Probes over different separation distances (S_d) as a function of magnetic latitude (λ) for (a) equatorial ($0° \leq \lambda \leq 5°$), (b) midlatitude ($5° \leq \lambda \leq 10°$), and (c) high latitude ($\lambda \geq 10°$) (caption of Figure 4 applies).

arrows, from Figures 6a to 6c, 2285 km, 2355 km, and 1545 km), resulting in steeper line of best fit marked with black lines (the correlation coefficients, from Figures 6a to 6c, are 0.036, 0.037, and 0 .077). This indicates that the two spacecraft are more likely to observe the same/similar chorus wave packets over a large S_d near the equator. By contrast, at higher latitudes the two spacecraft are only likely to observe the same/similar chorus wave packets when they are very closely separated. Also, the average ΔB beyond the saturation point varies with latitude. The average equatorial ΔB is 124 pT, average midlatitude ΔB is 117 pT, and average high-latitude ΔB is 103 pT. This is due to more intense chorus emissions near the equatorial source region [*Santolík et al.*, 2004; *Helliwell*, 1967].

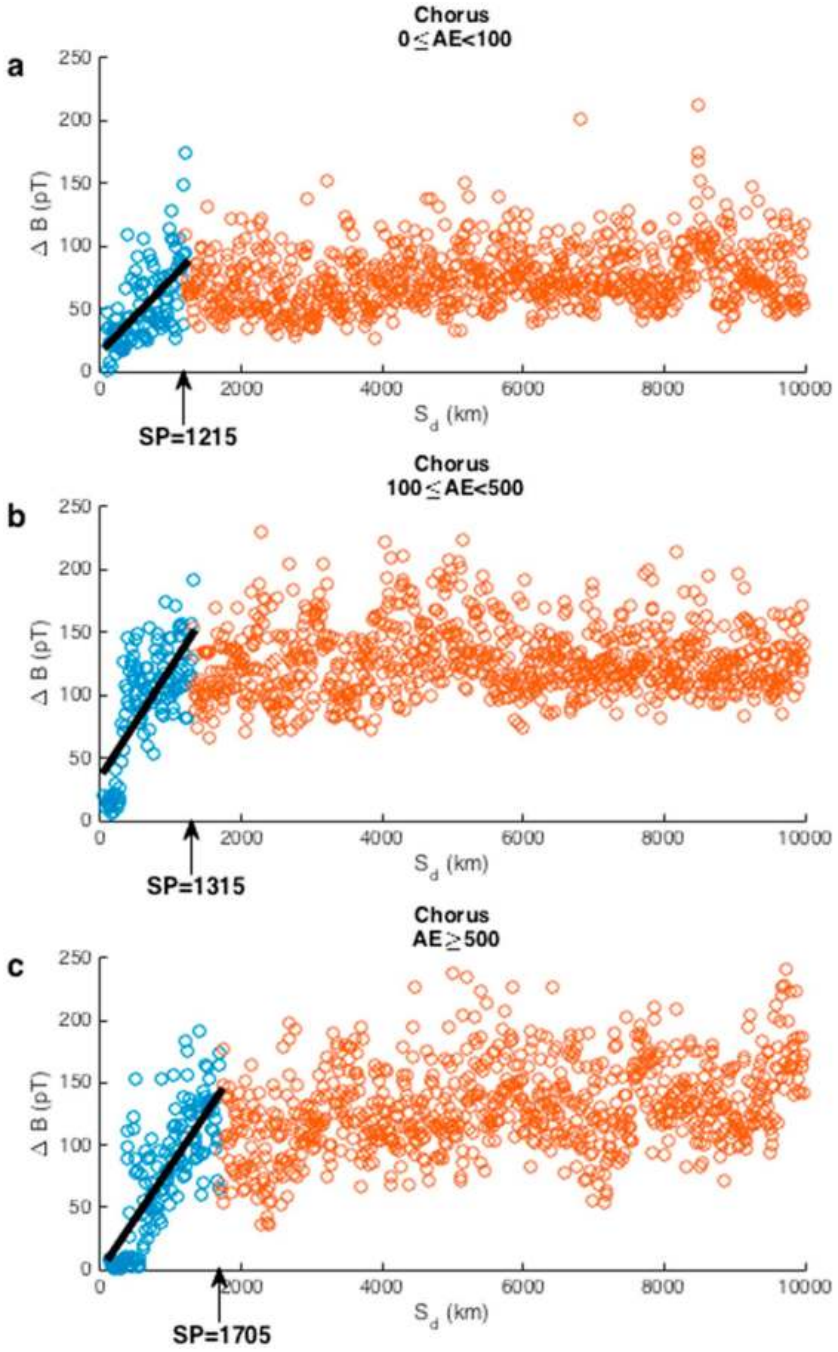

Figure 7. The difference between chorus wave amplitude (ΔB) observed by the two Van Allen Probes over different separation distances (S_d) as a function of geomagnetic activity for (a) quiet ($0 \leq AE \leq 300$), (b) moderate ($300 \leq AE \leq 500$), and (c) active ($AE \geq 500$) conditions (caption of Figure 4 applies).

Figure 7 illustrates the difference between the wave amplitude (ΔB) observed by the two Van Allen Probes over different separation distances as a function of geomagnetic activity for (a) quiet ($0 \leq AE < 300$), (b) moderate ($300 \leq AE < 500$), and (c) active ($AE \geq 500$) conditions. Results indicate that during active conditions the scale size of chorus wave packets is larger than during quiet conditions (marked with arrows, from Figures 7a to 7c, 1215 km, 1315 km, and 1705 km). Also, results show that the average ΔB beyond the saturation point varies with geomagnetic activity. The average ΔB during quiet, moderate, and active conditions are 75 pT, 128 pT, and 131 pT, respectively. This is due to higher chorus intensities during active conditions.

4. Conclusion

The present study examined almost 3 years (from September 2012 to end of May 2015) of EMFISIS data on board the two Van Allen Probes. The distribution of lower band chorus waves in the inner magnetosphere is presented as functions of combined geomagnetic index and solar wind parameters. The results show that combined parameter models provide better representation of the chorus wave distributions in the inner magnetosphere. In fact, the peak intensities of the combined geomagnetic index and B_s model during active conditions and high B_s are 14% larger than the peak intensities of the single parameter geomagnetic index during active conditions. Similarly, the peak intensities of the combined geomagnetic index and solar wind velocity model during active conditions and fast velocities are 17% larger than the peak intensities of the single parameter geomagnetic index during active conditions. This shows that the single parameter *AE* model alone can underestimate the average chorus intensities. Therefore, it is important to take into account the effect of solar wind parameters not only because combining solar wind parameters provide better representation of chorus wave distributions but also because solar wind parameters are directly measured. This can benefit studies of electron interaction with plasma waves, improve models that rely on the knowledge of chorus activity in the inner magnetosphere (such as the Comprehensive Inner Magnetosphere-Ionosphere (CIMI) model) [*Fok et al.*, 2014], and ultimately improve our knowledge of the acceleration and loss of radiation belt electrons.

The latter part of this study estimated the average scale size of chorus wave packets, during close separations between the two spacecraft, as a function of radial distance, magnetic latitude, and geomagnetic activity, respectively. Results illustrated that the two spacecraft observe the same/similar chorus wave packets when the separation distance between them is small. The difference between the wave amplitude (ΔB) observed by the two spacecraft increases as the two spacecraft move further apart up to a saturation point. Beyond the saturation point the two spacecraft do not observe the same/similar chorus wave packets. The location of the saturation point was used as an indication for the average scale size of chorus wave packets. Results indicated that chorus wave packets are larger near the equator, at lower radial distances, and during active conditions, respectively. The average scale size of chorus wave packets is generally between 1300 and 2300 km. This is comparable with previous studies, in particular, with the results of *Agapitov et al.* [2010]. Also the average ΔB beyond the saturation point is high near the equator and during active conditions due to more intense chorus activity. The estimated chorus wave packet scale sizes can help us understand the interaction region better and can allow us to compare theoretical predictions with the observations.

Acknowledgments

This study was supported by the NASA postdoctoral program. Portion of this work was supported by the Van Allen Probes program. We would also like to acknowledge NASA Grant NNX16AF85G. The authors would like to thank Alexa Halford, Kyle Murphy, Alexander Lipatov, and Quintin Schiller for their very useful science discussions. The EMFISIS waves data used in this study are available online (http://emfisis.physics.uiowa.edu/Flight/). The solar wind data were obtained by NASA's GSFC SPDF OMNIWEB and are also available online (http://omniweb.gsfc.nasa.gov).

References

Abel, B., and R. M. Thorne (1998), Electron scattering loss in Earth's inner magnetosphere 1. Dominant physical processes, *J. Geophys. Res.*, *103*, 2385–2396, doi:10.1029/97JA02919.

Agapitov, O., V. Krasnoselskikh, Y. Zaliznyak, V. Angelopoulos, O. Le Contel, and G. Rolland (2010), Chorus source region localization in the Earth's outer magnetosphere using THEMIS measurements, *Ann. Geophys.*, *28*, 1377–1386, doi:10.5194/angeo-28-1377-2010.

Agapitov, O., V. Krasnoselskikh, T. Dudok de Wit, Y. Khotyaintsev, J. S. Pickett, O. Santolík, and G. Rolland (2011), Multispacecraft observations of chorus emissions as a tool for the plasma density fluctuations' remote sensing, *J. Geophys. Res.*, *116*, A09222, doi:10.1029/2011JA016540.

Agapitov, O., A. Artemyev, V. Krasnoselskikh, Y. V. Khotyaintsev, D. Mourenas, H. Breuillard, M. Balikhin, and G. Rolland (2013), Statistics of whistler mode waves in the outer radiation belt: Cluster STAFF-SA measurements, *J. Geophys. Res. Space Physics*, *118*, 3407–3420, doi:10.1002/jgra.50312.

Agapitov, O. V., A. V. Artemyev, D. Mourenas, F. S. Mozer, and V. Krasnoselskikh (2015), Empirical model of lower band chorus wave distribution in the outer radiation belt, *J. Geophys. Res. Space Physics*, *120*, 10,425–10,442, doi:10.1002/2015JA021829.

Akasofu, S.-I., P. D. Perreault, F. Yasuhara, and C.-I. Meng (1973), Auroral substorms and the interplanetary magnetic field, *J. Geophys. Res.*, *78*, 7490–7508, doi:10.1029/JA078i031p07490.

Aryan, H., R. J. Boynton, and S. N. Walker (2013), Analysis of trends between solar wind velocity and energetic electron fluxes at geostationary orbit using the reverse arrangement test, *J. Geophys. Res. Space Physics*, *118*, 636–641, doi:10.1029/2012JA018216.

Aryan, H., K. Yearby, M. Balikhin, O. Agapitov, V. Krasnoselskikh, and R. Boynton (2014), Statistical study of chorus wave distributions in the inner magnetosphere using AE and solar wind parameters, *J. Geophys. Res. Space Physics*, *119*, 6131–6144, doi:10.1002/2014JA019939.

Baker, D. N., and S. G. Kanekal (2008), Solar cycle changes, geomagnetic variations, and energetic particle properties in the inner magnetosphere, *J. Atmos. Sol. Terr. Phys.*, *70*, 195–206, doi:10.1016/j.jastp.2007.08.031.

Baker, D. N., R. L. McPherron, T. E. Cayton, and R. W. Klebesadel (1990), Linear prediction filter analysis of relativistic electron properties at 6.6 R_E, *J. Geophys. Res.*, *95*, 15,133–15,140, doi:10.1029/JA095iA09p15133.

Baker, D. N., et al. (2014), Gradual diffusion and punctuated phase space density enhancements of highly relativistic electrons: Van Allen Probes observations, *Geophys. Res. Lett.*, *41*, 1351–1358, doi:10.1002/2013GL058942.

Beck, T. W., T. J. Housh, J. P. Weir, J. T. Cramer, V. Vardaxis, G. O. Johnson, J. W. Coburn, M. H. Malek, and M. Mielke (2006), An examination of the runs test, reverse arrangements test, and modified reverse arrangements test for assessing surface EMG signal stationarity, *J. Neurosci. Methods*, *156*(1-2), 242–248, doi:10.1016/j.jneumeth.2006.03.011.

Bendat, J. S., and A. G. Piersol (2000), *Random Data Analysis and Measurement Procedures*, pp. 96–99, Wiley, New York, doi:10.1088/0957-0233/11/12/702.

Bortnik, J., and R. M. Thorne (2007), The dual role of ELF/VLF chorus waves in the acceleration and precipitation of radiation belt electrons, *J. Atmos. Sol. Terr. Phys.*, *69*, 378–386, doi:10.1016/j.jastp.2006.05.030.

Bortnik, J., R. M. Thorne, and N. P. Meredith (2008), The unexpected origin of plasmaspheric hiss from discrete chorus emissions, *Nature*, *452*, 62–66, doi:10.1038/nature06741.

Bortnik, J., W. Li, R. M. Thorne, V. Angelopoulos, C. Cully, J. Bonnell, O. Le Contel, and A. Roux (2009), An observation linking the origin of plasmaspheric hiss to discrete chorus emissions, *Science*, *324*, 775–778, doi:10.1126/science.1171273.

Bortnik, J., L. Chen, W. Li, R. M. Thorne, Y. Nishimura, V. Angelopoulos, and C. A. Kletzing (2016), Relationship between chorus and plasmaspheric hiss waves, in *Low-Frequency Waves in Space Plasmas*, vol. 216, pp. 79–97, AGU, Washington, D. C., doi:10.1002/9781119055006.ch6.

Boynton, R. J., M. A. Balikhin, S. A. Billings, H. L. Wei, and N. Ganushkina (2011), Using the NARMAX OLS-ERR algorithm to obtain the most influential coupling functions that affect the evolution of the magnetosphere, *J. Geophys. Res.*, *116*, A05218, doi:10.1029/2010JA015505.

Burtis, W. J., and R. A. Helliwell (1969), Banded chorus—A new type of VLF radiation observed in the magnetosphere by OGO 1 and OGO 3, *J. Geophys. Res.*, *74*, 3002–3010, doi:10.1029/JA074i011p03002.

Burtis, W. J., and R. A. Helliwell (1976), Magnetospheric chorus—Occurrence patterns and normalized frequency, *Planet. Space Sci.*, *24*, 1007–1024, doi:10.1016/0032-0633(76)90119-7.

Cornilleau-Wehrlin, N., et al. (2005), The STAFF-DWP wave instrument on the DSP equatorial spacecraft: Description and first results, *Ann. Geophys.*, *23*, 2785–2801, doi:10.5194/angeo-23-2785-2005.

Davis, T. N., and M. Sugiura (1966), Auroral electrojet activity index AE and its universal time variations, *J. Geophys. Res.*, *71*, 785–801, doi:10.1029/JZ071i003p00785.

Fok, M.-C., N. Y. Buzulukova, S.-H. Chen, A. Glocer, T. Nagai, P. Valek, and J. D. Perez (2014), The comprehensive inner magnetosphere-ionosphere model, *J. Geophys. Res. Space Physics*, *119*, 7522–7540, doi:10.1002/2014JA020239.

Hamilton, D. C., G. Gloeckler, F. M. Ipavich, B. Wilken, and W. Stuedemann (1988), Ring current development during the great geomagnetic storm of February 1986, *J. Geophys. Res.*, *93*, 14,343–14,355, doi:10.1029/JA093iA12p14343.

Helliwell, R. A. (1967), A theory of discrete VLF emissions from the magnetosphere, *J. Geophys. Res.*, *72*, 4773–4790, doi:10.1029/JZ072i019p04773.

Hoffman, R. A., and J. L. Burch (1973), Electron precipitation patterns and substorm morphology, *J. Geophys. Res.*, *78*, 2867–2884, doi:10.1029/JA078i016p02867.

Horne, R. B., and R. M. Thorne (1998), Potential waves for relativistic electron scattering and stochastic acceleration during magnetic storms, *Geophys. Res. Lett.*, *25*, 3011–3014, doi:10.1029/98GL01002.

Horne, R. B., and R. M. Thorne (2003), Relativistic electron acceleration and precipitation during resonant interactions with whistler-mode chorus, *Geophys. Res. Lett.*, *30*, 1527, doi:10.1029/2003GL016973.

Horne, R. B., R. M. Thorne, S. A. Glauert, J. M. Albert, N. P. Meredith, and R. R. Anderson (2005), Timescale for radiation belt electron acceleration by whistler mode chorus waves, *J. Geophys. Res.*, *110*, A03225, doi:10.1029/2004JA010811.

Inan, U. S., M. Platino, T. F. Bell, D. A. Gurnett, and J. S. Pickett (2004), Cluster measurements of rapidly moving sources of ELF/VLF chorus, *J. Geophys. Res.*, *109*, A05214, doi:10.1029/2003JA010289.

Jordanova, V. K., et al. (1998), Effect of wave-particle interactions on ring current evolution for January 10–11, 1997: Initial results, *Geophys. Res. Lett.*, *25*, 2971–2974, doi:10.1029/98GL00649.

Kamide, Y., and J. D. Winningham (1977), A statistical study of the 'instantaneous' nightside auroral oval—The equatorward boundary of electron precipitation as observed by the Isis 1 and 2 satellites, *J. Geophys. Res.*, *82*, 5573–5588, doi:10.1029/JA082i035p05573.

Kennel, C. F., and H. E. Petschek (1966), Limit on stably trapped particle fluxes, *J. Geophys. Res.*, *71*, 1–28.

King, J. H., and N. E. Papitashvili (2005), Solar wind spatial scales in and comparisons of hourly Wind and ACE plasma and magnetic field data, *J. Geophys. Res.*, *110*, A02104, doi:10.1029/2004JA010649.

Kletzing, C. A., et al. (2013), The Electric and Magnetic Field Instrument Suite and Integrated Science (EMFISIS) on RBSP, *Space Sci. Rev.*, *179*, 127–181, doi:10.1007/s11214-013-9993-6.

Kullback, S. (1959), Information Theory and Statistics, Wiley Series in Probability and Mathematical Statistics, Probability and Mathematical Statistics John Wiley, New York.

Kullback, S., and R. A. Leibler (1951), On information and sufficiency, *Ann. Math. Stat.*, *22*, 79–86, doi:10.1214/aoms/1177729694.

Le Contel, O., et al. (2008), First results of the THEMIS search coil magnetometers, *Space Sci. Rev.*, *141*, 509–534, doi:10.1007/s11214-008-9371-y.

LeDocq, M. J., D. A. Gurnett, and G. B. Hospodarsky (1998), Chorus source locations from VLF Poynting flux measurements with the Polar spacecraft, *Geophys. Res. Lett.*, *25*, 4063–4066, doi:10.1029/1998GL900071.

Li, W., et al. (2009), Global distribution of whistler-mode chorus waves observed on the THEMIS spacecraft, *Geophys. Res. Lett.*, *36*, L09104, doi:10.1029/2009GL037595.

Li, W., J. Bortnik, R. M. Thorne, and V. Angelopoulos (2011), Global distribution of wave amplitudes and wave normal angles of chorus waves using THEMIS wave observations, *J. Geophys. Res.*, *116*, A12205, doi:10.1029/2011JA017035.

Li, W., et al. (2014), Radiation belt electron acceleration by chorus waves during the 17 March 2013 storm, *J. Geophys. Res. Space Physics*, *119*, 4681–4693, doi:10.1002/2014JA019945.

Li, X., D. N. Baker, M. Temerin, G. Reeves, R. Friedel, and C. Shen (2005), Energetic electrons, 50 keV to 6 MeV, at geosynchronous orbit: Their responses to solar wind variations, *Space Weather*, *3*, S04001, doi:10.1029/2004SW000105.

Li, X. F., and H.-R. Cho (1997), Development and propagation of equatorial waves, *Adv. Atmos. Sci.*, *14*, 323–338, doi:10.1007/s00376-997-0053-6.

Lui, A. T. Y., C. D. Anger, and S.-I. Akasofu (1975), The equatorward boundary of the diffuse aurora and auroral substorms as seen by the Isis 2 auroral scanning photometer, *J. Geophys. Res.*, *80*, 3603–3614, doi:10.1029/JA080i025p03603.

Lui, A. T. Y., S.-I. Akasofu, E. W. Hones Jr., S. J. Bame, and C. E. McIlwain (1976), Observation of the plasma sheet during a contracted oval substorm in a prolonged quiet period, *J. Geophys. Res.*, *81*, 1415–1419, doi:10.1029/JA081i007p01415.

Lyons, L. R., and R. M. Thorne (1973), Equilibrium structure of radiation belt electrons, *J. Geophys. Res.*, *78*, 2142–2149, doi:10.1029/JA078i013p02142.

Lyons, L. R., R. M. Thorne, and C. F. Kennel (1972), Pitch-angle diffusion of radiation belt electrons within the plasmasphere, *J. Geophys. Res.*, *77*, 3455–3474, doi:10.1029/JA077i019p03455.

Mauk, B. H., N. J. Fox, S. G. Kanekal, R. L. Kessel, D. G. Sibeck, and A. Ukhorskiy (2013), Science objectives and rationale for the radiation belt storm probes mission, *Space Sci. Rev.*, *179*, 3–27, doi:10.1007/s11214-012-9908-y.

Menvielle, M., and A. Berthelier (1991), The K-derived planetary indices—Description and availability, *Rev. Geophys.*, *29*, 415–432, doi:10.1029/91RG00994.

Meredith, N. P., R. B. Horne, A. D. Johnstone, and R. R. Anderson (2000), The temporal evolution of electron distributions and associated wave activity following substorm injections in the inner magnetosphere, *J. Geophys. Res.*, *105*, 12,907–12,918, doi:10.1029/2000JA900010.
Meredith, N. P., R. B. Horne, and R. R. Anderson (2001), Substorm dependence of chorus amplitudes: Implications for the acceleration of electrons to relativistic energies, *J. Geophys. Res.*, *106*, 13,165–13,178, doi:10.1029/2000JA900156.
Meredith, N. P., R. B. Horne, R. H. A. Iles, R. M. Thorne, D. Heynderickx, and R. R. Anderson (2002), Outer zone relativistic electron acceleration associated with substorm-enhanced whistler mode chorus, *J. Geophys. Res.*, *107*(A7), 1144, doi:10.1029/2001JA900146.
Meredith, N. P., R. B. Horne, R. M. Thorne, and R. R. Anderson (2003), Favored regions for chorus-driven electron acceleration to relativistic energies in the Earth's outer radiation belt, *Geophys. Res. Lett.*, *30*, 1871, doi:10.1029/2003GL017698.
Meredith, N. P., R. B. Horne, R. M. Thorne, D. Summers, and R. R. Anderson (2004), Substorm dependence of plasmaspheric hiss, *J. Geophys. Res.*, *109*, A06209, doi:10.1029/2004JA010387.
Meredith, N. P., R. B. Horne, A. Sicard-Piet, D. Boscher, K. H. Yearby, W. Li, and R. M. Thorne (2012), Global model of lower band and upper band chorus from multiple satellite observations, *J. Geophys. Res.*, *117*, A10225, doi:10.1029/2012JA017978.
Meredith, N. P., R. B. Horne, J. Bortnik, R. M. Thorne, L. Chen, W. Li, and A. Sicard-Piet (2013), Global statistical evidence for chorus as the embryonic source of plasmaspheric hiss, *Geophys. Res. Lett.*, *40*, 2891–2896, doi:10.1002/grl.50593.
Ni, B., R. M. Thorne, Y. Y. Shprits, and J. Bortnik (2008), Resonant scattering of plasma sheet electrons by whistler-mode chorus: Contribution to diffuse auroral precipitation,*Geophys. Res. Lett.*, *35*, L11106, doi:10.1029/2008GL034032.
Nishimura, Y., et al. (2010), Identifying the driver of pulsating aurora, *Science*, *330*, 81, doi:10.1126/science.1193186.
Nishimura, Y., et al. (2011), Multievent study of the correlation between pulsating aurora and whistler mode chorus emissions, *J. Geophys. Res.*, *116*, A11221, doi:10.1029/2011JA016876.
Omura, Y., M. Hikishima, Y. Katoh, D. Summers, and S. Yagitani (2009), Nonlinear mechanisms of lower-band and upper-band VLF chorus emissions in the magnetosphere, *J. Geophys. Res.*, *114*, A07217, doi:10.1029/2009JA014206.
Reeves, G. D., K. L. McAdams, R. H. W. Friedel, and T. P. O'Brien (2003), Acceleration and loss of relativistic electrons during geomagnetic storms, *Geophys. Res. Lett.*, *30*, 1529, doi:10.1029/2002GL016513.
Reeves, G. D., S. K. Morley, R. H. W. Friedel, M. G. Henderson, T. E. Cayton, G. Cunningham, J. B. Blake, R. A. Christensen, and D. Thomsen (2011), On the relationship between relativistic electron flux and solar wind velocity, *J. Geophys. Res.*, *116*, A02213, doi:10.1029/2010JA015735.
Reeves, G. D., S. Morley, and G. Cunningham (2013), Long-term variations in solar wind velocity and radiation belt electrons, *J. Geophys. Res. Space Physics*, *118*, 1040–1048, doi:10.1002/jgra.50126.
Roeder, J. L., J. F. Fennell, M. W. Chen, M. Schulz, M. Grande, and S. Livi (1996), CRRES observations of the composition of the ring-current ion populations, *Adv. Space Res.*, *17*, 17–24, doi:10.1016/0273-1177(95)00689-C.
Rostoker, G., E. Friedrich, and M. Dobbs (1997), Physics of magnetic storms, in *Magnetic Storms, Geophys. Monogr. Ser.*, *98*, pp. 149–160, AGU, Washington, D. C., doi:10.1029/GM098p0149.
Russell, C. T., and R. L. McPherron (1973), Semiannual variation of geomagnetic activity, *J. Geophys. Res.*, *78*, 92–108, doi:10.1029/JA078i001p00092.
Santolík, O. (2008), New results of investigations of whistler-mode chorus emissions, *Nonlinear Process. Geophys.*, *15*, 621–630.
Santolík, O., and D. A. Gurnett (2003), Transverse dimensions of chorus in the source region, *Geophys. Res. Lett.*, *30*, 1031, doi:10.1029/2002GL016178.
Santolík, O., D. Gurnett, and J. Pickett (2004), Multipoint investigation of the source region of storm-time chorus, *Ann. Geophys.*, *22*, 2555–2563, doi:10.5194/angeo-22-2555-2004.
Santolík, O., E. Macúšová, K. H. Yearby, N. Cornilleau-Wehrlin, and H. S. K. Alleyne (2005), Radial variation of whistler-mode chorus: First results from the STAFF/DWP instrument on board the Double Star TC-1 spacecraft, *Ann. Geophys.*, *23*, 2937–2942, doi:10.5194/angeo-23-2937-2005.
Santolík, O., et al. (2010), Wave-particle interactions in the equatorial source region of whistler-mode emissions, *J. Geophys. Res.*, *115*, A00F16, doi:10.1029/2009JA015218.
Santolík, O., C. A. Kletzing, W. S. Kurth, G. B. Hospodarsky, and S. R. Bounds (2014), Fine structure of large-amplitude chorus wave packets, *Geophys. Res. Lett.*, *41*, 293–299, doi:10.1002/2013GL058889.
Sazhin, S. S., and M. Hayakawa (1992), Magnetospheric chorus emissions—A review, *Planet. Space Sci.*, *40*, 681–697, doi:10.1016/0032-0633(92)90009-D.
Sheeley, B. W., M. B. Moldwin, H. K. Rassoul, and R. R. Anderson (2001), An empirical plasmasphere and trough density model: CRRES observations, *J. Geophys. Res.*, *106*, 25,631–25,642, doi:10.1029/2000JA000286.
Shprits, Y. Y., D. Subbotin, and B. Ni (2009), Evolution of electron fluxes in the outer radiation belt computed with the VERB code, *J. Geophys. Res.*, *114*, A11209, doi:10.1029/2008JA013784.
Shprits, Y. Y., A. Runov, and B. Ni (2013), Gyro-resonant scattering of radiation belt electrons during the solar minimum by fast magnetosonic waves, *J. Geophys. Res. Space Physics*, *118*, 648–652, doi:10.1002/jgra.50108.
Sugiura, M. (1963), *Hourly Values of Equatorial Dst for the IGY*, NASA, Goddard Space Flight Center, Greenbelt, Ottawa.
Summers, D., R. M. Thorne, and F. Xiao (1998), Relativistic theory of wave-particle resonant diffusion with application to electron acceleration in the magnetosphere, *J. Geophys. Res.*, *103*, 20,487–20,500, doi:10.1029/98JA01740.
Summers, D., C. Ma, N. P. Meredith, R. B. Horne, R. M. Thorne, D. Heynderickx, and R. R. Anderson (2002), Model of the energization of outer-zone electrons by whistler-mode chorus during the October 9, 1990 geomagnetic storm, *Geophys. Res. Lett.*, *29*(24), 2174, doi:10.1029/2002GL016039.
Summers, D., B. Ni, and N. P. Meredith (2007), Timescales for radiation belt electron acceleration and loss due to resonant wave-particle interactions: 2. Evaluation for VLF chorus, ELF hiss, and electromagnetic ion cyclotron waves, *J. Geophys. Res.*, *112*, A04207, doi:10.1029/2006JA011993.
Thomsen, M. F. (2004), Why *Kp* is such a good measure of magnetospheric convection, *Space Weather*, *2*, S11004, doi:10.1029/2004SW000089.
Thorne, R. M. (2010), Radiation belt dynamics: The importance of wave-particle interactions, *Geophys. Res. Lett.*, *37*, L22107, doi:10.1029/2010GL044990.
Thorne, R. M., T. P. O'Brien, Y. Y. Shprits, D. Summers, and R. B. Horne (2005), Timescale for MeV electron microburst loss during geomagnetic storms, *J. Geophys. Res.*, *110*, A09202, doi:10.1029/2004JA010882.
Thorne, R. M., B. Ni, X. Tao, R. B. Horne, and N. P. Meredith (2010), Scattering by chorus waves as the dominant cause of diffuse auroral precipitation, *Nature*, *467*, 943–946, doi:10.1038/nature09467.
Thorne, R. M., et al. (2013), Rapid local acceleration of relativistic radiation-belt electrons by magnetospheric chorus, *Nature*, *504*, 411–414, doi:10.1038/nature12889.

Tsurutani, B. T., and E. J. Smith (1974), Postmidnight chorus: A substorm phenomenon, *J. Geophys. Res.*, *79*, 118–127, doi:10.1029/JA079i001p00118.

Tsurutani, B. T., B. J. Falkowski, O. P. Verkhoglyadova, J. S. Pickett, O. SantolíK, and G. S. Lakhina (2012), Dayside ELF electromagnetic wave survey: A Polar statistical study of chorus and hiss, *J. Geophys. Res.*, *117*, A00L12, doi:10.1029/2011JA017180.

Turner, N. E., D. N. Baker, T. I. Pulkkinen, and R. L. McPherron (2000), Evaluation of the tail current contribution to Dst, *J. Geophys. Res.*, *105*, 5431–5440, doi:10.1029/1999JA000248.

Weygand, J. M., and E. Zesta (2008), Comparison of auroral electrojet indices in the Northern and Southern hemispheres, *J. Geophys. Res.*, *113*, A08202, doi:10.1029/2008JA013055.

Wing, S., et al. (2005), Kp forecast models, *J. Geophys. Res.*, *110*, A04203, doi:10.1029/2004JA010500.

Wygant, J. R., et al. (2013), The electric field and waves instruments on the radiation belt storm probes mission, *Space Sci. Rev.*, *179*, 183–220, doi:10.1007/s11214-013-0013-7.

Xiao, F., Z. Su, H. Zheng, and S. Wang (2009), Modeling of outer radiation belt electrons by multidimensional diffusion process, *J. Geophys. Res.*, *114*, A03201, doi:10.1029/2008JA013580.

Xiao, F., Z. Su, H. Zheng, and S. Wang (2010), Three-dimensional simulations of outer radiation belt electron dynamics including cross-diffusion terms, *J. Geophys. Res.*, *115*, A05216, doi:10.1029/2009JA014541.

Xiao, F., et al. (2015), Wave-driven butterfly distribution of Van Allen belt relativistic electrons, *Nat. Commun.*, *6*, 8590, doi:10.1038/ncomms9590.

Yagitani, S., T. Habagishi, and Y. Omura (2014), Geotail observation of upper band and lower band chorus elements in the outer magnetosphere, *J. Geophys. Res. Space Physics*, *119*, 4694–4705, doi:10.1002/2013JA019678.

Yearby, K. H., M. A. Balikhin, Y. V. Khotyaintsev, S. N. Walker, V. V. Krasnoselskikh, H. S. C. K. Alleyne, and O. Agapitov (2011), Ducted propagation of chorus waves: Cluster observations, *Ann. Geophys.*, *29*, 1629–1634, doi:10.5194/angeo-29-1629-2011.